Investigation of Filtering Algorithm for Noise Reduction in Displacement Sensing Signal

Changping Li, Ruining Huang, Ying Yi, and Amine Bermak, *Fellow, IEEE*

***Abstract*—With the emergence of new sensing technologies, soft substrate-based displacement sensing has gained popularity in the last decade. Nevertheless, performance degradation due to noise from unexpected vibrations of the substrate can affect the sensor's accuracy and lead to poor measurements. Few studies have focused on noise reduction to improve the accuracy of the sensing data. Based on mathematical modeling, this paper compares the two most representative filtering algorithms based on minimum mean square error (MMSE), namely recursive least squares (RLS) and Kalman algorithms for their predictive ability, accuracy, and reliability. Based on the modeling and comparison, we propose a Kalman filtering algorithm to suppress the vibration noise in the displacement-based dosage sensor. The filter-processed data from the sensor's measurement mainly contains the actual resistance change upon mechanical displacement of the sensor substrate and the undesired noise from its vibration. With the filtering algorithm, the noise can be reduced from the sensor's measurement, and an accurate correlation between resistance change and displacement of the sensor can be established. This would provide a straightforward sensing signal that reflects the displacement, and in turn, achieves precise dosage monitoring in drug delivery devices, which can be used as a test-bed application for the sensor.**

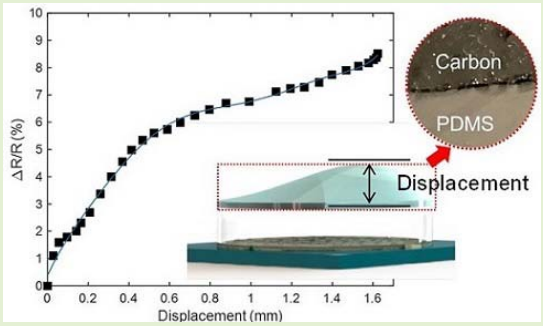

***Index Terms*— Displacement sensor, Kalman filtering algorithm, noise reduction.**

I. Introduction

FLEXIBLE substrate-based displacement sensors are becoming more popular due to their various applications, such as bridge displacement estimation [1] and structural health monitoring [2]. Nevertheless, the measured data from the sensor usually consist of actual values and the noise generated by different environmental conditions. For example, slight vibrations of the sensor substrate caused by the airflow can introduce measurement noise. Such noise can create estimation errors and inaccuracies at the system level. When such systems are used for structural health monitoring of super-tall buildings [3], for example, the estimation errors can lead to a greater risk of false alarms when relying only on the sensor's measurements. Therefore, a filter technique is required to reduce the noise in the sensor's measurements to improve accuracy.

Different filtering methods can be implemented either through hardware [4], [5] or software [6]. Using the hardware approach to filter the data is well known to increase the complexity and cost of the system, and present a risk in compatibility. Moreover, hardware-based filters add their own noise to the system. Instead, algorithm-based filtering approaches have become more common, because of their advantage due to their low-cost and simple deployment. Numerous filtering algorithms have been widely used for estimation [1], data fusion [3], interference cancellation [7], and noise reduction [8]. As a representative filter, the Kalman filtering algorithm, which uses the minimum mean square error (MMSE) [9] has been applied in many systems.

The Kalman filtering algorithm can rectify inaccurately measured values, while its accuracy varies according to its filter parameters, such as noise covariance. If the noise covariance is unknown or is roughly estimated (usually as an arbitrary value close to 0), the Kalman filter can lose its predictive ability [10]. Therefore, it is desirable to estimate the noise parameters of the measurement prior to the filtering operation. The maximum likelihood estimation [11] and wavelet transform [12] have been used to evaluate noise parameters, though they require a large set of parameters and involve complex

Manuscript received October 20, 2020; revised December 24, 2020; accepted December 27, 2020. Date of publication December 31, 2020; date of current version February 17, 2021. The associate editor coordinating the review of this article and approving it for publication was Prof. Aime Lay-Ekuakille. *(Corresponding author: Ying Yi.)*

Changping Li is with the College of Communication and Information Engineering, Chongqing University of Posts and Telecommunications, Chongqing 400065, China.

Ruining Huang is with the School of Mechanical Engineering and Automation, Harbin Institute of Technology, Shenzhen 518055, China.

Ying Yi and Amine Bermak are with the Division of Information and Computing Technology, College of Science and Engineering, Hamad Bin Khalifa University, Qatar Foundation, Doha 34100, Qatar (e-mail: yyi@hbku.edu.qa).

Digital Object Identifier 10.1109/JSEN.2020.3048511

denoising calculations. The accuracy of the filtered data is also important for specific applications, for example, an average percentage error of coordinates for acoustic emission sources should be detected within 5% after 10 iterations of the Kalman filter algorithm [13]. In the literature, the method used to verify the noise removal or to provide the specific accuracy of the filtered data is seldom reported [8].

In this paper, we propose a reliable method to estimate the accuracy of the noise reduction on a data set where the original values are known. More specifically, after applying the filtering algorithm to the noise-contaminated data sequence, the corresponding accuracy is obtained by comparing the filtered data with the original data. Besides accuracy, we also analyze and report on other performance metrics of the filter, including its predictive ability and reliability. We examined and compared the mathematical models of recursive least squares (RLS) and Kalman algorithms and found that the Kalman filter was superior to the RLS performance in terms of extracting the required signal from the measurements. We used a simple noise test to evaluate the measured noise variance so that the correct filter parameters could be used with the Kalman algorithm-based noise reduction for sensing data.

For the displacement-based dosage sensor, Figure 1(a)-(b) shows a diagram of an electrolytic actuator integrated with a piezoresistive sensor for drug delivery. Differing from the pressure sensor fabricated by mixing conductive nanoparticles into PDMS [14], our proposed sensor is fabricated by embedding solidified carbon ink into an elastic polydimethylsiloxane (PDMS) membrane [15] (Figure 1c). The displacement of the membrane, which is equal to the volume of the delivered drug, is caused by expansion of the electrolysis bubble [16]. When the electrolysis bubble-induced tension is applied to the membrane, the sensor outputs a resistance change ratio (ΔR). Because the membrane is soft and it can easily be observed to vibrate slightly in the measurement environment, the resulting sensing data involves measurement noise that contributes to an inaccurate dosage. By integrating the sensor with the Kalman filtering algorithm, our proposal aims to produce a more accurate noise-free measurement, which would improve the dosage monitoring of the drug delivery system.

II. Mathematical Model and Methodology

For a dynamic system, an accurate state or the desired data can be obtained with the Kalman filter algorithm using noisy measurements. The Kalman filter algorithm is a recursive process based on a state space model (SSM), which is presented in a linear stochastic difference equation:

$$\begin{cases} x_k = A_k x_{k-1} + B_k u_{k-1} + w_{k-1} \\ z_k = H_k x_k + v_k \end{cases} \tag{1}$$

where matrix A_k is a state transition matrix indicating the state x_{k-1} to the state x_k in the absence of either a driving function or process noise. The matrix B_k relates the optional control input u_k to the x_k. The matrix H_k relates the x_k to the measurement z_k. The random variables w_k and v_k are the process and measurement noises with covariance Q and R; they represent the uncertainty in the process model and the error source for the measurements, respectively.

A Kalman filtering cycle includes two recursive steps of the time and measurement updates for prediction and correction purposes, respectively. The initial conditions for the filter can be presented as:

$$E[x_0] = \hat{x}_0, \quad \text{and } E[(x_0 - \hat{x}_0)(x_0 - \hat{x}_0)^T] = P_0 \tag{2}$$

In the time update step, the estimation can be obtained by:

$$\begin{cases} \hat{x}_k^- = A\hat{x}_{k-1} + Bu_k \\ P_k^- = AP_{k-1}A^T + Q_k \end{cases} \tag{3}$$

where $\hat{x}_k^-$ is a priori state estimate at step k given the knowledge of the process prior to step k, and $\hat{x}_k$ is a posteriori estimate at step k, given measurement z_k. P_k^- is the covariance matrix of the prediction error.

In the measurement update step, the Kalman gain K_k and the estimation can be updated as:

$$\begin{cases} K_k = P_k^- H_k^T [H_k P_k^- H_k^T + R_k]^{-1} \\ \hat{x}_k = \hat{x}_k^- + K_k(z_k - H_k\hat{x}_k^-) \\ P_k = (I - K_k H_k) P_k^- \end{cases} \tag{4}$$

where K_k serves as an optimal weight between the prediction and the measurement. The $\hat{x}_k$ estimation is a recursive process via the MMSE calculation. The goal of the Kalman filtering algorithm is to obtain optimum filtered data by minimizing the trace of the P_k. When the P_k reaches its minimum value, the K_k is accordingly at the optimum, and the filtered data converges to the most accurate level.

As another popular MMSE-based interference cancellation technique, the RLS algorithm is selected for comparison. Differing from the Kalman filter, where the noise variance is required as a filter parameter, the RLS filter needs a training signal sequence to evaluate the channel state (or noise source) information. The ultimate goal of the RLS algorithm is to provide weight vector W estimates that minimize the error e between the original training sequence X and the received signal sequence Y at the filter. The weight vector of the filter and training sequence at k-th iteration is defined as:

$$W_k = [w_1, w_2, w_3, \ldots w_\rho] \tag{5}$$

and

$$\mathrm{X}_k = \begin{bmatrix} x_k \\ x_{k-1} \\ x_{k-2} \\ \vdots \\ x_{k-\rho+1} \end{bmatrix} \tag{6}$$

where ρ is the filter order. The RLS updates the weights recursively as follows:

$$\begin{cases} \mathrm{W_k} = \mathrm{W_{k-1}} + \mathrm{K_k e_k^*} \\ \mathrm{e_k} = \mathrm{X_k} - \mathrm{W_{k-1}^T Y_k} \\ \mathrm{K_k} = \mathrm{P_{k-1}^{-1} Y_k}[\lambda + \mathrm{Y_k^T P_{k-1}^{-1} Y_k}]^{-1} \\ \mathrm{P_k^{-1}} = \lambda^{-1}[\mathrm{P_{k-1}^{-1}} - \mathrm{K_k Y_k^T P_{k-1}^{-1}}] \end{cases} \tag{7}$$

where λ is a forgetting factor that represents a compromise between tracking ability and stability of the filtering algorithm.

Its value is usually within a range from 0.8 to 1 [6]. P^{-1} is a correlation matrix. As for the calculation, the initialization values of W_0, K_0 and X_0 are zero, and P_0^{-1} is an identity matrix. After obtaining a corresponding weight that reflects the channel state information, the RLS algorithm can filter the measurements z_k via $W_k^T z_k$.

To compare the performance of the Kalman and RLS algorithms in detail, their predictive ability, accuracy, and reliability were evaluated with different noise levels. In this work, noise level is defined as the ratio calculated by dividing the variance of noise by the variance of the tested signal. First, a normalized root mean square error (NRMSE) is selected to evaluate the prediction performance, calculated as:

$$\mathrm{NRMSE} = \frac{\sqrt{\sum_{i=1}^{N} (x_i - \hat{x}_i)}}{\sqrt{\sum_{i=1}^{N} (x_i - \tilde{x}_i)}} \tag{8}$$

where $\hat{x}_i$ and $\tilde{x}_i$ are the predicted and average values of the tested data sequence x_i. A value of the NRMSE close to zero indicates that the model exhibits perfect prediction, whereas a value greater than one implies that using the average value is better than the prediction of the model. The accuracy can be presented by the mean absolute error (MAE):

$$\mathrm{MAE} = \frac{\sum_{i=1}^{N} |x_i - \hat{x}_i|}{N} \tag{9}$$

where N is the total number in the test data sequence. Minimizing the difference $\varepsilon = |\hat{x}_i - x_i|$ is the aim of the noise reduction so that the filtered data will be much closer to the tested data and more accurate than the noisy data. For practical applications, a given accuracy is required or a limited error range is allowed. Once a value of ε is determined, a bit error rate (BER) is used to demonstrate the reliability of the model. The BER is the number of bit errors divided by the total number of streamed data, defined by $P(\hat{x}_i; |\hat{x}_i - x_i| \leq \varepsilon)$. Specifically, as long as $|\hat{x}_i - x_i| \leq \varepsilon$, the $\hat{x}_i$ can be regarded as a corrected bit.

Consider a noisy data sequence defined as $y_i = x_i + n$ where the corresponding noise-free data sequence, x_i, is randomized and known. The noise, n, is assumed to follow a Gaussian distribution. The filtered data sequence, $\hat{x}_i$, is compared to its original x_i at different noise levels using equations for the NRMSE, MAE, and BER. In the following calculations, we used a small value for Q to mitigate as much as possible the influence of process noise and to account for the fact that no process model is perfect and able to obtain a value of $Q = 0$. A forgetting factor of 0.99 and a filter order of 98 were used in the RLS algorithm to exhibit its best filtering performance, though at a cost of increased complexity of the system.

Figure 2 compares the performance metrics of the Kalman and RLS filtering algorithms. On the whole, the Kalman filtering is identified as a more predictable, accurate, and reliable approach compared to the RLS filtering, because the NRMSE, MAE and BER produced by the Kalman filter were lower than those produced by the RLS filter. The noise level is also easily seen to strongly affect the performance metrics of the algorithm. With an increasing noise level from 0.01% to 21%, the NRMSE produced by the Kalman filter logarithmically

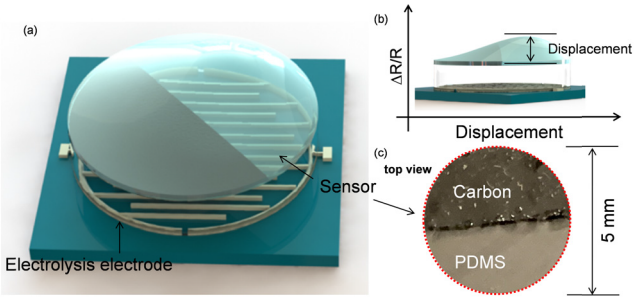

Fig. 1. (a) 3D diagram of the assembled electrolytic actuator integrated with a piezoresistive sensor; (b) definition of the mechanical displacement and sensor's output signal; (c) prototype of the sensor.

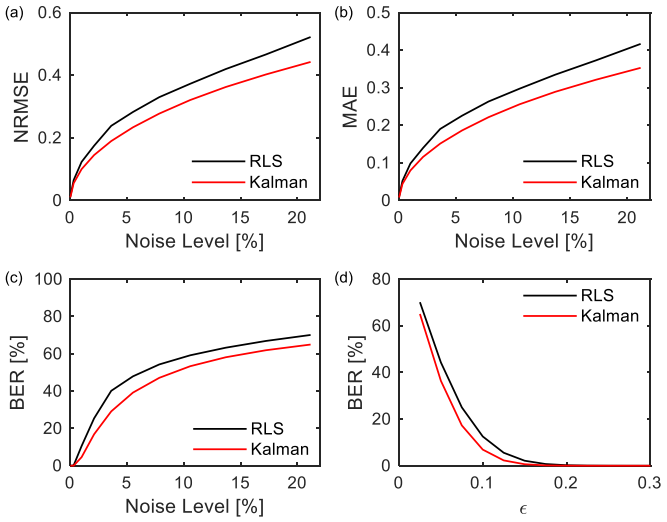

Fig. 2. Comparison of performance metrics for the Kalman and RLS filtering algorithms, in terms of (a) NRMSE, (b) MAE and (c-d) BER.

increased from 0.01 to 0.44 (Figure 2a). Similarly, the MAE exhibited a logarithmical growth to 0.35 (Figure 2b). With an assumed error difference, ε of 0.2, the BER produced by the Kalman filter sharply increased to 53% within the noise level up to 10.6%, while the BER increased steadily afterward (Figure 2c). A noise level of 0.3% was set as an example to demonstrate the compromise between accuracy and reliability. As expected, a decrease in the BER comes at the expense of allowing the ε to increase (Figure 2d). The BER exponentially decreased until ε reached a value of 0.14, beyond which the BER can be maintained below an ultra-low level (<1%).

III. Results and Discussion

The fabricated sensor that provided a resistance change as a function of the membrane's displacement was investigated. A digital multimeter was used to measure the resistance of the displacement sensor. The sensor's resistance was recorded in its non-tensile state under normal laboratory conditions for the purpose of noise testing. This correlated measurement of noise variance was used as a Kalman filter parameter. Varying resistance was observed, because airflow is hard to avoid in an engineering lab. The result was an undesired slight vibration of the sensor surface. This unwanted vibration

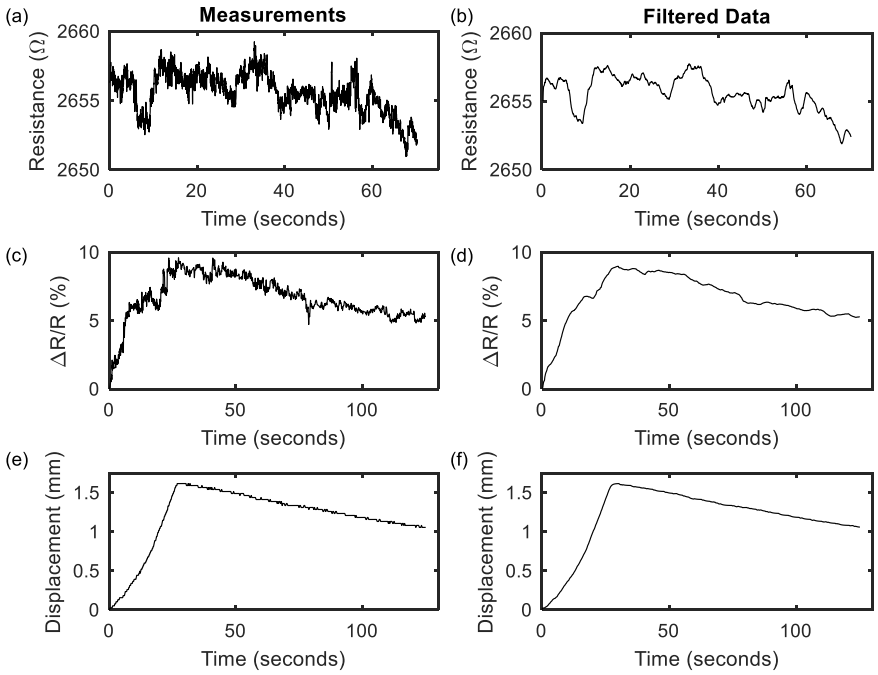

Fig. 3. Comparison of actual measurements (left) to filtered data (right), including (a-b) resistance, (c-d) delta R/R and (e-f) displacement.

was functioned as a major noise source in the resistance measurement. The noise covariance can be regarded as the R in the Kalman filtering algorithm. When power was applied to the electrolysis- electrode, electrolysis-induced bubbles were generated, causing an increase in pressure inside the electrolytic chamber. Consequently, the sensor membrane was deformed as an upward displacement. After removing the power, the electrolysis-bubbles recombined, causing a decreasing pressure inside the chamber, which was reflected by a downward displacement [16]. The displacement of the sensor membrane was detected by a laser Doppler vibrometer (LDV). Figure 3 compares the actual measurements (the graphs on the left) and the data filtered from the Kalman filter (the graphs on the right). The measurements included the noise test of the sensor (Figure 3a), the sensitivity of the sensor upon its displacement (Figure 3c), and an independent displacement measurement (Figure 3e). Using the covariance of the noise test results, the filtered data of the sensor in the lab environment is depicted in Figure 3(b), which shows a mean value of 2655 Ω with SD of ±2.4 Ω. Power of 4 mW was applied to the electrode for 30 seconds and then removed, and the resistance of the sensor changed (Figure 3c) in correspondence to its displacement (Figure 3e). The resistance noise and slight surface vibration of the sensor can be seen in the resistance and displacement measurements, respectively. With the Kalman filtering, the noise (or error) was reduced in the filtered data (Figure 3 (d) and (f)). Although the two sets of data exhibited similar characteristics, the filtered data formed a much smoother curve compared to the original measurements due to the significant noise reduction, thereby improving the accuracy. In the above Kalman filtering algorithm, the trace of the error covariance matrix was examined to clarify the convergence of the filter. Figure 4 shows the trace of the error covariance. The sum of squared errors reached its minimum

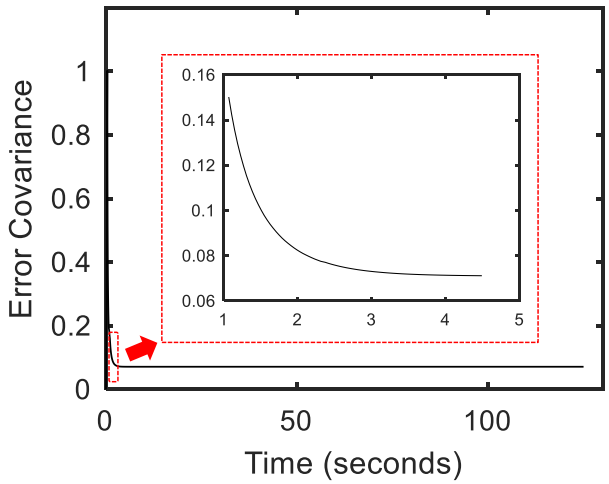

Fig. 4. Trace of the error covariance.

level in about 3 seconds, which implies that the Kalman gain was determined for the data from the sensor after 3 seconds.

Because the displacement and resistance of the sensor membrane were measured by two different instruments, the correlation of the displacement and resistance change (ΔR/R-displacement curve) is hard to accomplish if the noise is not reduced. With the Kalman filtering algorithm, the correlation of the filtered displacement and ΔR/R data is plotted in Figure 5, demonstrating the sensitivity of the sensor upon displacement. In the "power on" period, the ΔR/R exhibited a logarithmic growth with an increase in displacement. It rapidly increased at the beginning, which was followed by a period where the growth slowed down until reaching a maximum of 8.5% at a displacement of 1.6 mm. This outcome is reasonable, because the resistance of the sensor

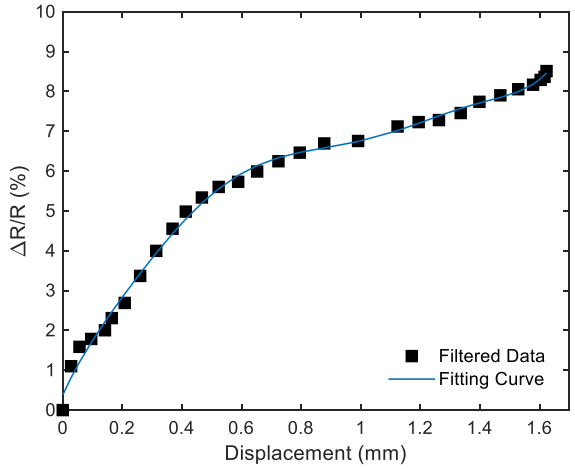

Fig. 5. The filtered resistance change ratio of the sensor as a function of displacement.

changes in correspondence to the deformation volume of the membrane. The deformation of the sensor membrane is similar to a conical shape. The beginning displacement would cause a large deformation volume of the sensor membrane; however, the growth of the volume would decelerate with the displacement. To summarize, depending on the covariance of the measurement in the noise test that acted as a filtering parameter, the Kalman filter maintained excellent noise reduction for displacement sensing data.

IV. Conclusion

Attempts to use a filtering algorithm to reduce the noise in displacement sensing data are rarely seen. In this paper, we evaluated the performance metrics of the Kalman filter algorithm, including its predictive ability, accuracy, and reliability, and applied it to reduce the measurement noise for the purpose of improving accuracy. The noise test for the displacement sensor was implemented to provide the covariance of the measurement noise, which was used as a filtering parameter of the Kalman algorithm. In our results, the filtered data reflected similar characteristics to the original measured data, though it was more convincing and accurate. Moreover, with the filtering algorithm, the correlation between the displacement and the signal output of the sensor was easier to establish, which lies at the core of the dosage monitoring sensing function.

References

[1] M. Z. Sarwar and J.-W. Park, "Bridge displacement estimation using a co-located acceleration and strain," *Sensors*, vol. 20, no. 4, p. 1109, Feb. 2020, doi: 10.3390/s20041109.

[2] Y. Yi, B. Wang, and A. Bermak, "A low-cost strain gauge displacement sensor fabricated via shadow mask printing," *Sensors*, vol. 19, no. 21, p. 4713, Oct. 2019, doi: 10.3390/s19214713.

[3] H. Zhu *et al.*, "Multi-rate data fusion for dynamic displacement measurement of beam-like supertall structures using acceleration and strain sensors," *Struct. Health Monitor.*, vol. 19, no. 2, pp. 520–536, Mar. 2020, doi: 10.1177/1475921719857043.

[4] A. Chabuda, P. Durka, and J. Zygierewicz, "High frequency SSVEP-BCI with hardware stimuli control and phase-synchronized comb filter," *IEEE Trans. Neural Syst. Rehabil. Eng.*, vol. 26, no. 2, pp. 344–352, Feb. 2018, doi: 10.1109/tnsre.2017.2734164.

[5] J. Li, B. Yu, W. Zhao, and W. Chen, "A review of signal enhancement and noise reduction techniques for tunable diode laser absorption spectroscopy," *Appl. Spectrosc. Rev.*, vol. 49, no. 8, pp. 666–691, Nov. 2014, doi: 10.1080/05704928.2014.903376.

[6] Y. Yi, C. Li, and K. Lee, "Adaptive MMSE equalizer for optical multipath dispersion in indoor visible light communication," *IETE J. Res.*, vol. 58, no. 5, p. 347, 2012, doi: 10.4103/0377-2063.104150.

[7] Y. Yi, C. Li, and K. Lee, "Wavelength division-adaptive interference cancellation applied in OFDM visible light communication systems," *IETE J. Res.*, vol. 58, no. 5, p. 390, 2012, doi: 10.4103/0377-2063.104157.

[8] D. S. K. Karunasingha and S.-Y. Liong, "Enhancement of chaotic hydrological time series prediction with real-time noise reduction using extended Kalman filter," *J. Hydrol.*, vol. 565, pp. 737–746, Oct. 2018, doi: 10.1016/j.jhydrol.2018.08.044.

[9] Y. Ma and T. J. Lim, "The Kalman filter as the optimal linear minimum mean-squared error multiuser CDMA detector," *IEEE Trans. Inf. Theory*, vol. 46, no. 7, pp. 2561–2566, Nov. 2000, doi: 10.1109/18.887863.

[10] S. Park, M. Gil, H. Im, and Y. Moon, "Measurement noise recommendation for efficient Kalman filtering over a large amount of sensor data," *Sensors*, vol. 19, no. 5, p. 1168, 2019, doi: 10.3390/s19051168.

[11] Y. Xu, J. M. W. Brownjohn, D. Hester, and K. Y. Koo, "Long-span bridges: Enhanced data fusion of GPS displacement and deck accelerations," *Eng. Struct.*, vol. 147, pp. 639–651, Sep. 2017, doi: 10.1016/j.engstruct.2017.06.018.

[12] K. Mets, F. Depuydt, and C. Develder, "Two-stage load pattern clustering using fast wavelet transformation," *IEEE Trans. Smart Grid*, vol. 7, no. 5, pp. 2250–2259, Sep. 2016, doi: 10.1109/tsg.2015.2446935.

[13] L. Morse, Z. S. Khodaei, and M. H. Aliabadi, "Reliability based impact localization in composite panels using Bayesian updating and the Kalman filter," *Mech. Syst. Signal Process.*, vol. 99, pp. 107–128, Jan. 2018, doi: 10.1016/j.ymssp.2017.05.047.

[14] A. Massaro, F. Spano, A. Lay-Ekuakille, P. Cazzato, R. Cingolani, and A. Athanassiou, "Design and characterization of a nanocomposite pressure sensor implemented in a tactile robotic system," *IEEE Trans. Instrum. Meas.*, vol. 60, no. 8, pp. 2967–2975, Aug. 2011, doi: 10.1109/TIM.2011.2121290.

[15] Y. Yi, A. Samara, and B. Wang, "A new approach for an ultra-thin piezoresistive sensor based on solidified carbon ink film," *J. Mater. Sci.*, vol. 56, no. 1, pp. 607–614, Jan. 2021, doi: 10.1007/s10853-020-05309-8.

[16] Y. Yi, U. Buttner, and I. G. Foulds, "A cyclically actuated electrolytic drug delivery device," *Lab Chip*, vol. 15, no. 17, pp. 3540–3548, 2015, doi: 10.1039/c5lc00703h.